

The computed S_1 reaction path involves passage over the transition state h^* followed by return to the ground state via a fully efficient decay through the conical intersection region i^* near prebenzvalene d . This reaction path is consistent with a channel 3 decay mechanism (loss of fluorescence^{8,11-13} above the critical threshold of 3000 cm^{-1} or 8.6 kcal mol^{-1}) that corresponds to photochemical conversion of the excited molecule to the isomeric benzvalene and also with the photochemical observation² that the quantum yield of benzvalene is wavelength dependent. (Dynamics calculations indicate that decay through a conical intersection occurs within one vibrational period³⁷.) The computed nonadiabatic coupling and gradient difference vectors give some rationalization of the experimental observation that the disappearance of observed fluorescence is not accompanied² by a significant rise in the (small) quantum yield of benzvalene. While one of the two vectors that lift the degeneracy corresponds to motion along the benzene-to-fulvene interconversion coordinate, the other corresponds to motion along the interconversion coordinate between two localized Kekule structures and leads to a high-energy out-of-plane distorted Kekule valence bond structure and back to benzene itself. Further, the flat nature of the ground-state surface in the prefulvene region $b-c-d-e$ implies that topological control of the reaction is lost. There is almost no barrier on a reaction from the prebenzvalene intermediate d back to benzene itself.

The surprising aspect of benzene photochemistry is related to S_2 . Our results show that the different photochemistry attributed to S_2 is, in fact, not due to S_2 directly at all, since the crossing to S_1 is fully efficient via the conical intersection j^{**} of S_2/S_1 . Rather, the occurrence of Dewar benzene as a product of S_2 photochemistry is due to the fact that the S_0/S_1 crossing surface will be entered at the region k^* , well above the minimum l^* of the S_0/S_1 crossing surface, with a geometry that can be a precursor of either Dewar benzene or benzvalene. In other words, k^* and l^* lie on the same $(n-2)$ -dimensional S_0/S_1 crossing surface. This result is consistent with experimental observations²⁰ that both

benzvalene and Dewar benzene may be produced via selective population of S_2 and S_3 . With initial energies sufficient only to overcome the barrier on S_1 , only benzvalene is produced via the mechanism described above. When there is an excess of energy (decay from higher excited states), the system has access to higher energy points on the S_0/S_1 crossing surface with different geometries, yielding a wider distribution of products subsequent to decay. It must be noted that the molecules returning to the ground state at such points will be extremely "hot" and efficient relaxation channels will be necessary for the system to relax into the high-energy valence isomer minima. Thus, one does not observe Dewar benzene from benzene vapor-phase photolysis.

In this work we have demonstrated that the products of benzene photochemistry appear to be controlled by the topology of the S_0/S_1 crossing surface. While we have only fully optimized the minimum of this crossing surface, we have also been able to demonstrate that this surface is accessible in the region of the S_1/S_2 crossing minimum. Thus, the photochemistry must depend on the energy used in the experiment (and thus dynamical considerations) and the detailed topology of this crossing surface. This conjecture has some experimental support in the fact that in substituted^{2,5} or site perturbed benzenes⁴⁶ one observes different photoproducts. In hexafluorobenzene, the Dewar benzene isomer is the major product of photolysis from S_2 , with fluorescence occurring from S_1 . In an argon matrix⁴⁶ where benzene is "site perturbed", one observes Dewar benzene via photolysis with a source of 253.7 nm.

Acknowledgment. This research has been supported by the SERC (U.K.) under Grant No. GR/G 03335. Ian Palmer is grateful to the SERC (U.K.) for the award of a studentship. The authors are also grateful to IBM for support under a Joint Study Agreement. All computations were run on an IBM RS/6000.

(46) Johnstone, D. E.; Sodeau, J. R. *J. Phys. Chem.* 1991, 95, 165-169.

Electron Donor-Acceptor Complexes as Potential High-Efficiency Second-Order Nonlinear Optical Materials. A Computational Investigation

Santo Di Bella,[†] Ignazio L. Fragalá,[†] Mark A. Ratner,* and Tobin J. Marks*

Contribution from the Department of Chemistry and the Materials Research Center, Northwestern University, Evanston, Illinois 60208-3113. Received March 16, 1992

Abstract: The second-order nonlinear optical response of model molecular 1:1 and asymmetric 2:1 organic π electron donor-acceptor (EDA) complexes is investigated using the INDO/S sum-over-excited particle-hole-states formalism. It is found that intermolecular charge-transfer transitions in EDA complexes represent a promising approach to achieving sizable second-order optical nonlinearities. Calculated hyperpolarizabilities may be generally related to the strength of the donor-acceptor interaction in the complex, affording for a given acceptor, the largest values in the case of aminoarene donors. The large change in dipole moment that accompanies intermolecular charge-transfer transitions and the relatively low-lying charge-transfer excitation energies are the major sources of the large calculated second-order nonlinearities. The relative orientation of donor and acceptor components is also an important feature, leading to stabilization of the ground state as well as to maximization of the oscillator strength of the lowest energy charge-transfer excitation and, in turn, the NLO response. In the case of asymmetric 2:1 EDA complexes, calculated hyperpolarizability enhancements over the 1:1 complexes can be related to the red-shift of the charge-transfer excitation as well as to an increase in dipole moment change between ground and excited states. The perturbation theoretical "two-level" model is a useful first approximation for predicting the second-order nonlinear response of such complexes.

Introduction

An indispensable prerequisite for achieving large second-order nonlinear optical (NLO) response in molecular chromophores is the existence of strong intramolecular charge-transfer (CT) ex-

citations.¹ This can be understood in terms of perturbation theoretical arguments,¹ which consider the effect of an oscillating

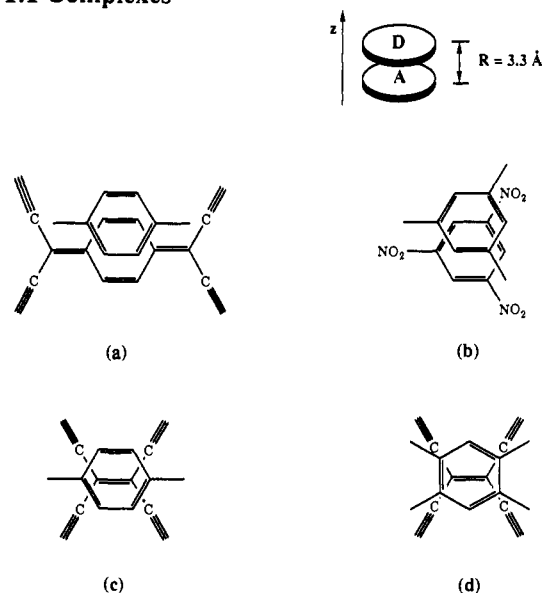
[†] Permanent address: Dipartimento di Scienze Chimiche, Università di Catania, 95125 Catania, Italy.

(1) (a) Boyd, R. W. *Nonlinear Optics*; Academic Press: New York, 1992. (b) Prasad, P. N.; Williams, D. J. *Introduction to Nonlinear Optical Effects in Molecules and Polymers*; Wiley: New York, 1991. (c) Shen, Y. R. *The Principles of Nonlinear Optics*; Wiley: New York, 1984.

electric field on the molecule. The field mixes the excited states into the ground state, leading to charge separation and polarization, the magnitude of which can be related to the extent of charge transfer. Extensive efforts have been directed toward the design and synthesis of new molecular chromophores having optimized donor/acceptor substituents and conjugated connecting pathways to maximize intramolecular CT transitions and, in turn, the second-order NLO response.^{1,2} An alternative approach to achieving substantial NLO responses might be to construct molecular systems possessing intermolecular CT transitions. This possibility is offered by organic π electron donor-acceptor (EDA) complexes, known to possess intense, low-energy excitations involving substantial charge redistribution from the electron donor (D) molecule to the electron acceptor (A) molecule of the complex.³ Furthermore, these transitions are accompanied by a large change in the dipole moment between ground and excited states,³ so that an appreciable second-order NLO response might be expected.⁴

Among the known organic EDA complexes,^{3,5} those formed by cofacial interaction of substituted aromatic rings seem the most attractive, because they might be readily incorporated into covalently functionalized glassy polymers^{1,6,7} or into chromophoric self-assembled architectures^{8,9} or might offer possible alternatives to present classes of NLO chromophores.¹⁰ In this regard, a chemically-oriented, computationally efficient theoretical analysis capable of probing the microscopic NLO characteristics of EDA complexes would be of great importance in designing and eval-

1:1 Complexes



2:1 Complexes

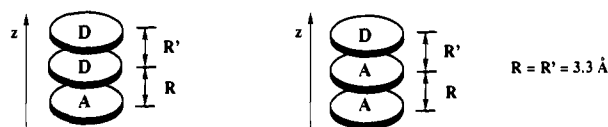
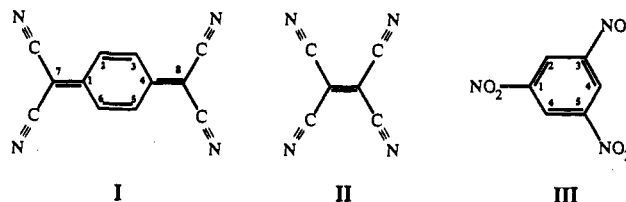


Figure 1. Molecular geometries of the types of EDA complexes examined in this study: 7,7,8,8-tetracyanoquinodimethane (TCNQ)-para-substituted arene (a), 1,3,5-trinitrobenzene (TNB)-1,3,5-trisubstituted arene (b), tetracyanoethylene (TCNE)-para-substituted arene (c), and TCNE-1,2,4,5-tetraminobenzene (d).

uating synthetic strategies for new types of efficient NLO materials.

In this contribution we explore, using the proven INDO-SOS quantum chemical formalism, the second-order nonlinear response $\beta(-2\omega; \omega, \omega)$ and analyze β -determining architectural parameters in 1:1 and asymmetric 2:1 EDA model complexes (Figure 1). We focus on archetypical π -acceptor molecules such as 7,7,8,8-tetracyanoquinodimethane (TCNQ, I), tetracyanoethylene (TCNE, II), and 1,3,5-trinitrobenzene (TNB, III), interacting with arene molecules having various electron-donating groups (methyl, methoxy, amine) as substituents.



Computational Details

The sum-over-excited particle-hole-states (SOS) formalism,¹¹ in connection with the all-valence INDO/S (intermediate neglect of differential overlap) model,¹² was employed in the present study. Details of the computationally-efficient ZINDO-SOS-based method for accurately describing second-order molecular optical nonlinearities have been reported elsewhere.¹³ The INDO/S model has been successfully used for

(11) Ward, J. F. *Rev. Mod. Phys.* **1965**, *37*, 1.

(12) (a) Anderson, W. P.; Edwards, W. D.; Zerner, M. C. *Inorg. Chem.* **1986**, *25*, 728. (b) Bacon, A. D.; Zerner, M. C. *Theor. Chim. Acta (Berlin)* **1979**, *53*, 21. (c) Ridley, J.; Zerner, M. C. *Theor. Chim. Acta (Berlin)* **1973**, *32*, 111.

(2) (a) *Materials for Nonlinear Optics: Chemical Perspectives*; Marder, S. R., Sohn, J. E., Stucky, G. D., Eds.; ACS Symposium Series 455, Washington, DC, 1991. (b) *Nonlinear Optical Properties of Organic Materials IV*; Singer, K. D., Ed.; SPIE Proc. 1991; Vol. 1560. (c) *Nonlinear Optical Properties of Organic Materials III*; Khanarian, G., Ed.; SPIE Proc. 1990; Vol. 1337. (d) *Nonlinear Optical Properties of Organic Materials II*; Khanarian, G., Ed.; SPIE Proc. 1990; Vol. 1147. (e) *Nonlinear Optical Effects in Organic Polymers*; Messier, J., Kajar, F., Prasad, P., Ulrich, D., Eds.; Kluwer Academic Publishers: Dordrecht, 1989. (f) *Organic Materials for Nonlinear Optics*; Hann, R. A., Bloor, D., Eds.; Royal Society of Chemistry: London, 1988. (g) *Nonlinear Optical Properties of Organic Molecules and Crystals*; Chemla, D. S., Zyss, J., Eds.; Academic Press: New York, 1987; Vols. 1 and 2. (h) *Nonlinear Optical Properties of Organic and Polymeric Materials*; Williams, D. J., Ed.; ACS Symposium Series 233; Washington, DC, 1984.

(3) (a) Mulliken, R. S.; Person, W. B. *Molecular Complexes. A Lecture and Reprint Volume*; Wiley: New York, 1969. (b) Foster, R. *Organic Charge-Transfer Complexes*; Academic Press: New York, 1969. (c) *Molecular Complexes*; Foster, R., Ed.; Elek, Science: London, 1973; Vol. 1; 1974; Vol. 2.

(4) For an early example in which SHG was used to detect the formation of 1, charge-transfer complexes in solution see: (a) Levine, B. F.; Bethea, C. G. *J. Chem. Phys.* **1976**, *65*, 2439. (b) Levine, B. F.; Bethea, C. G. *J. Chem. Phys.* **1977**, *66*, 1070.

(5) Kochi, J. K. *Pure Appl. Chem.* **1991**, *63*, 255 and references therein.

(6) Pearson, J. M.; Turner, S. R. In *Molecular Association, Including Molecular Complexes*; Foster, R., Ed.; Academic Press: New York, 1979; p 79.

(7) (a) Dai, D.-R.; Hubbard, M. A.; Li, D.; Park, J.; Ratner, J. A.; Marks, T. J.; Yang, J.; Wong, G. K. in ref 2a p 226 and references therein. (b) Dai, D.-R.; Marks, T. J.; Yang, J.; Lundquist, P. M.; Wong, G. K. *Macromolecules* **1990**, *23*, 1894. (c) Ye, C.; Minami, N.; Marks, T. J.; Yang, J.; Lundquist, P. M.; Wong, G. K. in ref 2f, p 263. (d) Ye, C.; Minami, N.; Marks, T. J.; Yang, J.; Wong, G. K. *Macromolecules* **1988**, *21*, 2901. (e) Ye, C.; Marks, T. J.; Yang, J.; Wong, G. K. *Macromolecules* **1987**, *20*, 2322.

(8) (a) Köhler, W.; Robello, D. R.; Willand, C. S.; Williams, D. J. *Macromolecules* **1991**, *24*, 4689 and references therein. (b) Chen, M.; Yu, L.; Dalton, L. R.; Shi, Y.; Steier, W. H. *SPIE Proc.* **1991**, *1409*, 202-213. (c) Eich, M.; Sen, A.; Looser, H.; Bjorklund, G. C.; Swalen, J. D.; Twieg, R.; Yoon, D. Y. *J. Appl. Phys.* **1989**, *66*, 2559. (d) Singer, K. D.; Kuzyk, M. G.; Holland, W. R.; Sohn, J. E.; Lalama, S. J.; Commizzoli, R. B.; Katz, H. E.; Schilling, M. L. *Appl. Phys. Lett.* **1988**, *53*, 1800.

(9) (a) Li, D.; Ratner, M. A.; Marks, T. J.; Zhang, C.; Yang, J.; Wong, G. K. *J. Am. Chem. Soc.* **1990**, *112*, 7389. (b) Li, D.; Marks, T. J.; Zhang, C.; Yang, J.; Wong, G. K. in ref 2c, p 341. (c) Katz, H. E.; Scheller, G.; Putvinski, T. J.; Schilling, M. L.; Wilson, W. L.; Chidsey, C. E. D. *Science* **1991**, *254*, 1485-1487. (d) Allan, D. S.; Kubota, F.; Marks, T. J.; Zhang, T. J.; Lin, W. P.; Wong, G. K. in ref 2b, p 362. (e) Allan, D. S.; Kubota, F.; Orihaski, Y.; Li, D.; Marks, T. J.; Zhang, T. G.; Lin, W. P.; Wong, G. K. *Polym. Preprints* **1991**, *32*, 86.

(10) For a recent example of a third-order NLO material based upon an organic EDA complex, see: Gotoh, T.; Kondoh, T.; Egawa, K.; Kubodera, K. *J. Opt. Soc. Am. B* **1989**, *6*, 703.

the description of molecular linear¹² and nonlinear^{13,14} optical responses as well as for the linear optical properties of various intermolecular interactions,¹⁵ including those in EDA complexes.¹⁶ Standard parameters and basis functions were used. In the present approach, the single-determinant, molecular orbital approximate ground state was used, and the monoexcited configuration interaction (MECI) approximation was employed to describe the excited states. In all of the present computations, the 130 lowest energy transitions between SCF and MECI electronic configurations were chosen to undergo CI mixing and were included in the SOS. This SOS truncation was found to be sufficient for a complete convergence of the second-order response in all cases considered.

Stabilization of moderate to strong EDA complexes is largely determined by charge-transfer interactions and, to a lesser extent, by electrostatic and dispersion effects.^{17,18} The latter term is important in determining the equilibrium geometry of the complex. Nevertheless, for computing the hyperpolarizabilities of the present EDA complexes having fixed structures, the INDO/S model should be suitable because charge-transfer and electrostatic interactions are taken into account. Both of these contributions are essential for the description of dipole moments and linear optical phenomena, hence for the NLO response.

Geometrical parameters for calculations on 1:1 EDA complexes were taken from published crystallographic data^{19,20} or from the structures of the neutral donor and acceptor molecular constituents.²¹ The geometries of 1:1 EDA complexes were constructed assuming cofacial conformations where the molecular planes are parallel and the principal rotation axes are coincident (Figure 1). Considering all donor and acceptor molecular components to possess D_{2h} or D_{3h} symmetry, the resulting complexes are of C_{2v} or C_{3v} symmetry, respectively. These conformations, for each class of EDA complex, are very close to those found in related crystallographic studies.^{19,20} For all 1:1 EDA complexes studied, the intermolecular D-A distance was chosen to be 3.30 Å. This distance represents the average experimental interplanar spacing value found for all these classes of EDA complexes^{19,20} and suffices to illustrate key points of the β -determining intermolecular interactions. Geometries of asymmetric, ADD or AAD, complexes were constructed starting from those of 1:1 complexes and adding a donor or acceptor molecule in a cofacial conformation so that the resulting complexes possessed the same symmetry as the 1:1 complexes. The intermolecular distance was assumed to be the typical^{19,20} 3.30 Å spacing.

Results and Discussion

1:1 EDA Complexes. Table I summarizes calculated dipole moment, linear optical, and second-order hyperpolarizability data for selected 1:1 cofacial EDA complexes (see Figure 1 for structures). Calculated dipole moments range from 0.5 to 1.5 Debyes, and their magnitude reflects the degree of charge-transfer interaction in the ground state,^{3,18} i.e., the strength of the EDA complex. As expected, the dipole moment increases with increasing donor strength and, in each series, becomes maximum in the case of the aminoarene donor. An analogous trend is observed in the lowest energy CT transition, which becomes

Table I. Calculated Dipole Moment, Linear Optical Spectroscopic, and Molecular Hyperpolarizability $\beta(-2\omega; \omega, \omega)$ Data^a (10^{-30} cm⁵ esu⁻¹; $\hbar\omega = 0.65$ eV) for Cofacial 1:1 Electronic Donor-Acceptor Complexes Involving Various Electron Acceptor Molecules (A)

donor ^b (D)	μ^c (Debyes)	$\hbar\omega_{ge}^{c,d}$ (eV)	f^c	$\Delta\mu_{ge}^c$ (Debyes)	β_{zzz}^c	β_{1zzz}^e
A = TCNQ						
TMDP	1.07	2.04	0.14	14.43	68.36	69.96
PD	1.04	2.33	0.14	14.46	39.01	38.50
DMB	0.40	3.02	0.08	14.29	8.39	7.77
PX	0.60	3.27	0.11	13.75	9.08	8.04
HMB	0.68	3.03	0.11	14.04	11.06	10.23
A = TCNE						
TTAB	1.33	2.04	0.14	14.54	68.51	69.08
PD	0.83	2.45	0.10	14.94	23.22	22.78
DMB	0.54	3.25	0.09	14.98	8.23	7.79
PX	0.62	3.48	0.11	14.95	7.28	6.97
HMB	0.59	3.37	0.12	15.65	9.34	8.95
A = TNB						
TAB	0.59	2.29	0.06	14.46	21.95	18.97
TRIAZ	0.36	3.00	0.06	15.03	11.18	7.10

^a For definition of parameters see text. ^b TMDP = *N,N,N',N'*-tetramethyl-*p*-phenylenediamine, PD = *p*-phenylenediamine, DMB = 1,4-dimethoxybenzene, PX = *p*-xylene, HMB = hexamethylbenzene, TTAB = 1,2,4,5-tetraaminobenzene, TAB = 1,3,5-triaminobenzene, TRIAZ = 2,4,6-tris(dimethylamino)-1,3,5-triazine. ^c Calculated using the INDO/S SOS formalism. ^d Lowest energy CT transition. ^e Calculated using the simple two-level model of eq 1.

stronger (increasing oscillator strength, f) and shifted to lower energy as the donor strength increases.

Unfortunately, the paucity of experimental vapor-phase dipole moment and optical absorption data for EDA pairs precludes extensive quantitative comparisons with the present calculated data. Furthermore, the possibility of multiple structural conformations,^{3,22} the formation of 2:1 complexes,^{3,23} and solvation interactions which generally stabilize the excited state more than the ground state (leading to a red shift of absorption spectra on passing from vapor-phase to solution^{3,24}) render a meaningful comparison of our calculated data with the available experimental solution absorption spectra impracticable. Nevertheless, the previous successes of the present computational formalism¹²⁻¹⁶ make us confident that key NLO trends for EDA complexes will be accurately described.

Calculated $\beta_{zzz}(-2\omega; \omega, \omega)$ values (Table I) may be roughly related to the strength of the EDA complexes and range from $\sim 8 \times 10^{-30}$ cm⁵ esu⁻¹ ($\hbar\omega = 0.65$ eV), similar to that reported for *p*-nitroaniline,¹³ to $\sim 70 \times 10^{-30}$ cm⁵ esu⁻¹ ($\hbar\omega = 0.65$ eV), rivaling those reported for efficient second-order NLO chromophores such as DANS.¹³ As expected, analysis of contributions to β_{zzz} reveals that the NLO response in all complexes examined is largely determined by the lowest energy CT excitation. In terms of perturbation theory, this means that a single CT term dominates the perturbation sum. The two-level model²⁵ for β (eq (1)) should consequently be a suitable guideline for rationalizing the NLO response of EDA complexes. Here β_i is the two-level hyperpo-

$$\beta_i(-2\omega; \omega, \omega) = \frac{3e^2}{2} \frac{\omega_{ge} f \Delta\mu_{ge}}{[(\hbar\omega_{ge})^2 - (\hbar\omega)^2][(\hbar\omega_{ge})^2 - (2\hbar\omega)^2]} \quad (1)$$

larizability term, $\Delta\mu_{ge}$ the difference between excited- and

(13) (a) Kanis, D. R.; Ratner, M. A.; Marks, T. J.; Zerner, M. A. *Chem. Mater.* **1991**, *3*, 19. (b) Kanis, D. R.; Ratner, M. A.; Marks, T. J. *J. Am. Chem. Soc.* **1990**, *112*, 8203. (c) Kanis, D. R.; Ratner, M. A.; Marks, T. J. *Int. J. Quant. Chem.* **1992**, *43*, 61.

(14) (a) Parkinson, W. A.; Zerner, M. C. *J. Chem. Phys.* **1991**, *94*, 478. (b) Ulman, A.; Willand, C. S.; Kohler, W.; Robello, D. R.; Williams, D. J.; Handley, L. *J. Am. Chem. Soc.* **1990**, *112*, 7083.

(15) (a) Thompson, M. A.; Zerner, M. C. *J. Am. Chem. Soc.* **1991**, *113*, 8210. (b) Thompson, M. A.; Zerner, M. C.; Fajer, J. *J. Phys. Chem.* **1991**, *95*, 5693. (c) Canuto, S.; Zerner, M. C. *J. Am. Chem. Soc.* **1990**, *112*, 2114.

(16) Edwards, W. D.; Du, M.; Royal, J. S.; McHale, J. L. *J. Phys. Chem.* **1990**, *94*, 5748.

(17) Morokuma, K.; Kitaura, K. In *Molecular Interactions*; Ratajczak, H., Orville Thomas, W. J., Redshaw, M., Eds.; Wiley & Sons: New York, 1980; Vol. 1, p 21.

(18) (a) Glauser, W. A.; Raber, D. J.; Stevens, B. *J. Phys. Chem.* **1989**, *93*, 1784. (b) Glauser, W. A.; Raber, D. J.; Stevens, B. *J. Comp. Chem.* **1988**, *9*, 539.

(19) (a) Mayoh, B.; Prout, C. K. *J. Chem. Soc., Faraday Trans. II* **1972**, *68*, 1072. (b) Herbstein, F. H. In *Perspectives in Structural Chemistry*; Dunitz, J. D., Ibers, J. A., Eds.; Wiley: New York, 1971; Vol. IV, p 166.

(20) (a) Saheki, M.; Yamada, H.; Yoshioka, H.; Nakatsu, K. *Acta Crystallogr. B* **1976**, *32*, 662. (b) Iwasaki, F.; Saito, Y. *Acta Crystallogr. B* **1970**, *26*, 251. (c) Williams, R. M.; Wallwork, S. C. *Acta Crystallogr.* **1966**, *21*, 406. (d) Hanson, A. W. *Acta Crystallogr.* **1965**, *19*, 610.

(21) (a) Little, R. G.; Pautler, D.; Coppens, P. *Acta Crystallogr. B* **1971**, *27*, 1493. (b) Long, R. E.; Sparks, R. A.; Trueblood, K. N. *Acta Crystallogr.* **1965**, *18*, 932.

(22) (a) Frey, J. E.; Cole, R. D.; Kitchen, E. C.; Suprenant, L. M.; Sylwestrzak, M. S. *J. Am. Chem. Soc.* **1985**, *107*, 748. (b) Mobley, M. J.; Rieckhoff, K. E.; Voigt, E. M. *J. Phys. Chem.* **1978**, *82*, 2005.

(23) (a) Merriam, M. J.; Rodriguez, R.; McHale, J. L. *J. Phys. Chem.* **1987**, *91*, 1058. (b) Smith, M. L.; McHale, J. L. *J. Phys. Chem.* **1985**, *89*, 4002.

(24) Mataga, N.; Kubota, T. *Molecular Interactions and Electronic Spectra*; Dekker, Inc.: New York, 1970.

(25) (a) Oudar, J. L. *J. Chem. Phys.* **1977**, *67*, 446. (b) Oudar, J. L.; Chémia, D. S. *J. Chem. Phys.* **1977**, *66*, 2664.

ground-state dipole moments, $\hbar\omega$ the incident radiation frequency, and $\hbar\omega_{ge}$ the energy, and f , the oscillator strength of the optical transition ($\lambda_{max} = 2\pi c/\omega_{ge}$) involved in the two-level process. Since the charge-transfer transition has a dominant contribution along the z axis (Figure 1), the β_i term should be largely proportional to the β_{zzz} tensor, so that $\beta_i(-2\omega; \omega, \omega) \approx \beta_{i,zzz}$. As can be seen in Table I, the estimated two-level $\beta_{i,zzz}$ terms are quantitatively comparable to the calculated SOS β_{zzz} values so that a simplified physical analysis of variables influencing β_{zzz} should be straightforward.

All of the present EDA complexes are characterized by large, almost constant changes in the dipole moment between the first excited and ground states ($\Delta\mu_{ge}$), so that the β_i values may be simply related to $\hbar\omega_{ge}$ and f , the optimization of which is crucial for the design of efficient NLO EDA complexes. In particular, the hyperpolarizability will be very sensitive to the energy of the CT transition. For a given acceptor, the energy of the lowest energy CT transition may be simply related to the donor strength, affording lower $\hbar\omega_{ge}$ values in the case of amine-substituted donors, hence larger hyperpolarizabilities. On the other hand, transparency considerations vis-à-vis practical laser sources impose some limits in the molecular design. All hyperpolarizability data reported in Table I are for an off-resonant input frequency of 0.65 eV. For higher energy laser frequencies (e.g., $\hbar\omega = 1.16$ eV) more significant resonant enhancement is expected. In these cases, the simple SOS treatment is inadequate since damping corrections must be taken into account.¹

The relative orientation and orbital overlap between donor and acceptor constituents is the most important feature leading to charge-transfer stabilization of EDA complexes in both ground and excited states.³ In particular, the simplified analysis of frontier orbitals (LUMO for the acceptor and HOMO for the donor) is useful for understanding the charge-transfer interaction in the ground state as well as for maximizing the oscillator strength of the lowest energy CT transition. In a simple Mulliken two-state model,³ the ground (Ψ_g)- and excited (Ψ_e)-state wave functions are described by a linear combination of no-bond $\Psi(D,A)$ and ionic $\Psi(D^+,A^-)$ states (eqs 2 and 3) where $a \gg b$.²⁶ The state

$$\Psi_g = a\Psi_0(D,A) + b\Psi_1(D^+,A^-) \quad (2)$$

$$\Psi_e = a\Psi_1(D^+,A^-) - b\Psi_0(D,A) \quad (3)$$

Ψ_1 differs from Ψ_0 by the promotion of an electron from the donor HOMO, ϕ_D , to the acceptor LUMO, ϕ_A . The b coefficient, the square of which is a measure of the amount of charge transfer, is proportional to the overlap integral between ϕ_D and ϕ_A . The transition moment of the lowest energy CT transition, μ_{ge} , may be approximated by eq 4 (using eqs 2 and 3) where μ_{00} and μ_{11}

$$\mu_{ge} = ab(\mu_{11} - \mu_{00}) + (a^2 - b^2)\mu_{01} \quad (4)$$

are the dipole moments of the no-bond and covalent states and μ_{01} is the transition moment between the two states. The first term ($\mu_{11} - \mu_{00}$) corresponds to the variation in the dipole moment produced by transferring an electron from D to A and is large. The second term may be related to the overlap integral between ϕ_D and ϕ_A . Therefore μ_{ge} and f ($f = \text{constant} \cdot \nu_{ge}(\mu_{ge})^2$) become larger with an increasing contribution of charge-transfer character in the ground state (in terms of the b coefficient) as well as with increasing orbital overlap between D and A. Both conditions require that the HOMO, ϕ_D , and the LUMO, ϕ_A , must be of the same symmetry in the point group of the complex, and both μ_{ge} and f are maximized when these MOs are strongly overlapping.

For a given acceptor in the present EDA complexes, the energy of the supermolecular LUMO as well as its atomic population are found to be almost constant, i.e., independent of the donor molecule. In contrast, the energy of the HOMO in the complex²⁷

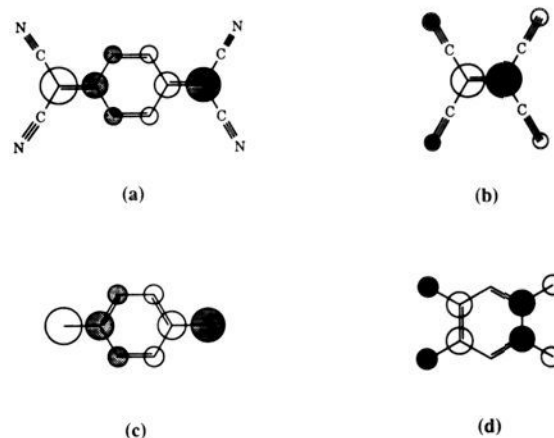


Figure 2. Frontier orbitals of selected EDA complexes: LUMO of TCNQ (a) and TCNE (b) complexes, HOMO of TCNQ-*N,N,N',N'*-tetramethyl-*p*-phenylenediamine (c), and TCNE-1,2,4,5-tetraamino-benzene (d) complexes.

Table II. Calculated Dipole Moment, Linear Optical Spectroscopic, and Molecular Hyperpolarizability $\beta(-2\omega; \omega, \omega)$ Data^a (10^{-30} cm⁵ esu⁻¹; $\hbar\omega = 0.65$ eV) for Cofacial Asymmetric ADD Electronic Donor–Acceptor Complexes Involving Various Electron Acceptor Molecules (A)

donor ^b (D)	μ^c (Debyes)	$\hbar\omega_{ge}^{c,d}$ (eV)	f^c	$\Delta\mu_{ge}^c$ (Debyes)	β_{zzz}^c	$\beta_{i,zzz}^e$
A = TCNQ						
TMDP	1.42	1.77	0.16	18.29	188.44	199.52
PD	1.25	2.02	0.15	18.63	89.85	95.92
DMB	0.50	2.64	0.08	18.62	16.78	17.38
PX	0.75	2.78	0.11	18.91	20.82	20.80
HMB	0.91	2.58	0.11	19.04	26.29	27.25
A = TCNE						
TTAB	1.63	1.85	0.16	17.29	148.25	152.75
PD	0.10	2.19	0.11	17.88	49.03	50.17
DMB	0.64	2.99	0.11	16.81	13.75	13.26
PX	0.74	3.01	0.11	19.20	14.76	15.40
HMB	0.80	2.73	0.12	19.74	22.34	23.27
A = TNB						
TAB	0.71	1.93	0.06	18.57	57.32	45.26

^a For definition of parameters see text. ^b TMDP = *N,N,N',N'*-tetramethyl-*p*-phenylenediamine, PD = *p*-phenylenediamine, DMB = 1,4-dimethoxybenzene, PX = *p*-xylene, HMB = hexamethylbenzene, TTAB = 1,2,4,5-tetraaminobenzene, TAB = 1,3,5-triaminobenzene. ^c Calculated using the INDO/S SOS formalism. ^d Lowest energy CT transition. ^e Calculated using the simple two-level model of eq 1.

is strongly modulated by electron donating substituents on the donor aromatic ring. In the case of the TCNQ complexes, the LUMO is of b_{2g} symmetry (in a local D_{2h} point group), the electronic distribution of which is largely localized at the 1, 4, 7, and 8 atomic positions (Figure 2a). Consequently, a donor molecule having a HOMO of the same symmetry and having two electron donating substituents in 1–4 positions is expected to have an optimum overlap (Figures 1a and 2a), thus a large f . In the case of TCNE complexes (Figure 2b), the same arguments indicate that overlap maximization may be achieved in the same fashion as the TCNQ complexes or, better, with an arene donor molecule having four substituents in 1, 2, 4, and 5 positions such as the 1,2,4,5-tetraaminobenzene (Figures 1d and 2d). In each case, the trend of calculated f values (Table I) accords with these qualitative symmetry considerations, and maximum f values occur

(26) The formulation of Ψ_e , where a single configuration is included, is valid here since in almost all of the present EDA complexes, the lowest energy CT transition essentially involves a single configuration, resulting from the composition of the CI expansion.

(27) In the case of relatively strong EDA complexes, such as *p*-xylene-TCNQ, the SHOMO (second highest occupied MO) is involved in the lowest energy CT transition.

Table III. Calculated Dipole Moment, Linear Optical Spectroscopic, and Molecular Hyperpolarizability $\beta(-2\omega; \omega, \omega)$ Data^a (10^{-30} cm⁵ esu⁻¹; $\hbar\omega = 0.65$ eV) for Cofacial Asymmetric AAD Electronic Donor-Acceptor Complexes Involving Various Electron Acceptor Molecules (A)

donor ^b (D)	μ^c (Debyes)	$\hbar\omega_{ge}^{c,d}$ (eV)	f^c	$\Delta\mu_{ge}^c$ (Debyes)	β_{zzz}^c	$\beta_{1,zzz}^e$
A = TCNQ						
TMDP	1.44	1.77	0.16	17.35	187.92	194.86
PD	1.26	2.05	0.15	17.24	80.68	83.54
DMB	0.47	2.69	0.07	16.27	13.09	11.47
PX	0.67	2.94	0.09	16.03	13.25	11.59
HMB	0.88	2.70	0.09	16.67	17.28	16.37
A = TCNE						
TTAB	1.63	1.81	0.15	16.91	150.73	157.88
PD	0.96	2.20	0.10	16.84	40.24	41.58
DMB	0.61	2.99	0.09	16.66	11.38	11.30
PX	0.69	3.22	0.10	16.63	9.87	9.86
HMB	0.71	3.13	0.12	15.70	12.16	11.71
A = TNB						
TAB	0.71	2.05	0.05	15.42	38.50	22.80

^a For definition of parameters see text. ^b TMDP = *N,N,N',N'*-tetramethyl-*p*-phenylenediamine, PD = *p*-phenylenediamine, DMB = 1,4-dimethoxybenzene, PX = *p*-xylene, HMB = hexamethylbenzene, TTAB = 1,2,4,5-tetraaminobenzene, TAB = 1,3,5-triaminobenzene. ^c Calculated using the INDO/S SOS formalism. ^d Lowest energy CT transition. ^e Calculated using the simple two-level model of eq 1.

for donors with amino electron donating substituents.

Asymmetric 2:1 EDA Complexes. Let us now consider the second-order NLO response in asymmetric 2:1 EDA complexes (Figure 1). The formation of ADD EDA complexes has been achieved in cyclophane molecules containing rigidly constrained donor and acceptor moieties.²⁸ Formation of ADD or AAD complexes has also been reported in functionalized EDA polymeric structures.⁶

As expected, formation of 2:1 ADD or AAD complexes (Figure 1) leads to increasing calculated dipole moments (Tables I-III) that may be related to more extensive charge-transfer interactions in the ground state. Furthermore, the lowest energy CT transitions are red-shifted compared to those of the 1:1 analogues. Experimental observation of red-shifting of CT transitions in asymmetric 2:1 EDA complexes^{23,29} supports our theoretical analysis. In ADD

complexes, the lowest energy CT transition in the CI expansion involves, to various extents, a combination of HOMO and SHOMO, both localized in the DD moiety, and the LUMO. The latter has essentially the same energy and atomic population found in 1:1 complexes. The red-shift of the CT transition can be simply related to the energy splitting of the HOMO and SHOMO due to the DD interaction. An analogous situation occurs in AAD complexes, where the lowest energy CT transition involves the HOMO and a combination of LUMO and SLUMO.

For all 2:1 EDA cases considered, a substantial increase of β_{zzz} compared to that of the 1:1 analogues, more marked for the strong complexes, is observed (Tables II and III). It can also be seen that the simple two-level approximation is still a good model in predicting the NLO response. Therefore, within the previous two-level model arguments, the hyperpolarizability enhancement in asymmetric 2:1 EDA complexes may be essentially related to the red-shift of the lowest energy CT transition and, to smaller extent, to the increase of $\Delta\mu_{ge}$ (Tables II and III). In both the ADD and AAD complexes, the previously discussed symmetry and overlap constraints must be satisfied to obtain strong transitions, even though little increase of the oscillator strength is expected (Tables II and III). Qualitatively, the red-shifted transition can be understood in terms of spectator stabilization pictures, in which the polarization of a third entity (the extra D or A in ADD or AAD triplexes, respectively) stabilizes the excited CT state.

Conclusions

The results of this investigation indicate that intermolecular charge-transfer excitations between cofacially arrayed molecular donors and acceptors can, under favorable conditions, lead to microscopic frequency doubling responses comparable to, or perhaps even greater than, those due to strong intramolecular donor-acceptor substituents. Such results clearly suggest some attractive alternative approaches to the synthesis of materials with large second-order optical nonlinearities. These are currently under investigation.

Acknowledgment. This research was supported by the NSF-MRL program through the Material Research Center of Northwestern University (Grant DMR8821571), by the Air Force Office of Scientific Research (Contract 90-0071), and by the Italian Consiglio Nazionale della Ricerche (CNR, Rome, Progetto Finalizzato Materiali avanzati). S.D.B. also thanks the CNR for a postdoctoral fellowship. We thank Dr. D. Kanis for ongoing collaborations.

(28) Misumi, S. In *Cyclophanes*; Kechn P. M., Rosenfeld, S. M., Eds.; Academic Press: New York, 1983; Vol. 11, p 573.

(29) Gribaudo, M. L.; Knorr, F. J.; McHale, J. L. *Spectrochim. Acta, Part A* 1985, 41, 419.